2014

Experimental Demonstration of Model Predictive Control in a Medium-Sized Commercial Building

Pengfei Li
United Technologies Research Center, United States of America, lip1@utrc.utc.com

Dapeng Li
United Technologies Research Center, United States of America, lid1@utrc.utc.com

Draguna Vrabie
United Technologies Research Center, United States of America, vrabiedl@utrc.utc.com

Sorin Bengea
United Technologies Research Center, United States of America, bengeasc@utrc.utc.com

Stevo Mijanovic
United Technologies Research Center, United States of America, MijanoS@UTRC.utc.com

Experimental Demonstration of Model Predictive Control in a Medium-Sized Commercial Building

Pengfei LI[1]*, Dapeng LI, Draguna VRABIE, Sorin BENGEA, Stevo MIJANOVIC

[1] United Technologies Research Center,
East Hartford, CT, USA
(Phone: 860-610-7215, Fax: 860-557-8709, E-mail: lip1@utrc.utc.com)

* Corresponding Author

ABSTRACT

This paper presents the implementation and experimental demonstration results of a practically effective and computationally efficient model predictive control (MPC) algorithm used to optimize the energy use of the heating, ventilation, and air-conditioning (HVAC) system in a multi-zone medium-sized commercial building. Advanced building control technologies are key enablers for intelligent operations of future buildings, however, adopting these technologies are quite difficult in practice mainly due to the cost-sensitive nature of the building industry. This paper presents the results of implementing optimization-based control algorithm and demonstrates the effectiveness of its energy-saving feature and improved thermal comfort along with lessons-learned. The performance of the implemented MPC algorithm was estimated relative to baseline days (heuristic-based control) with similar outdoor air temperature patterns during the cooling and shoulder seasons (September to November, 2013), and it was concluded that MPC reduced the total electrical energy consumption by more than 20% on average while improving thermal comfort in terms of temperature and maintaining similar zone CO_2 levels.
Keywords: *Model Predictive Control, Energy Efficient Buildings, Experimental Demonstration*

1. INTRODUCTION

Commercial and residential buildings together account for 40 quads (41%) of primary energy consumption in the United States (DOE 2010). Improved building energy efficiency can directly result in significant reduction of energy consumption, carbon emission, and utility expenses. Among the efforts to address this issue, advanced building control has shown efficiency improvements through better coordination of various HVAC components, adaption to environmental changes and elimination of human errors. Current building controls are typically based on a decentralized architecture. For example, the air handling unit (AHU) has its own control mission to satisfy supply air temperature setpoint and variable air volume (VAV) units are controlled to meet their flow setpoints to maintain zone temperature. Advanced building controls such as optimization-based control, however, tends to bridge the subsystem operation together and leverage the trade-offs between HVAC components (Brambley *et al*., 2005, Katipamula *et al*., 2012).

One candidate of advanced control methodologies is Model Predictive Control (MPC). Since its inception, MPC has been deeply rooted in control practices and has borne fruit in areas such as process control, motion control and many more. For a detailed survey one is referred to Qin and Badgwell (2003). Thanks to its proven benefits such as prediction and constraint management, MPC has been studied by the HVAC community with a number of experimental results including optimizing building operation with a large water storage tank (Ma *et al.* 2009), optimizing low-lift chiller for thermo-active building systems (Gayeski, 2010), optimizing building heating systems (Siroký *et al.*, 2011), optimization of conventional HVAC systems in a full-scale building (Narayanan, 2011; Bengea *et al.*, 2014), multi-objective optimization scheme for commercial offices (West *et al.*, 2014), and radiant cooled building (May-Ostendorp *et al.* 2013).

This work focused on demonstrating control strategy development, model calibration & validation, algorithm deployment, and benefit analysis. Building on the simulation work (Li *et al*., 2012) published previously, this work demonstrates MPC performance in a real-life medium-sized commercial building. The MPC algorithm is also tailored to accommodate some practical considerations.

The paper is organized as follows. Part 2 will introduce the demonstration building at Philadelphia Navy Shipyard. The implementation details of MPC algorithm will be presented in Part 3 and followed by MPC performance evaluation against baseline in Part 4.

2. BUILDING 101 AT PHILADELPHIA NAVY YARD

The demonstration building is a medium-sized commercial building (Building 101) located at the Philadelphia Navy Shipyard. The gross area of the building is 75,156 ft^2 with 65,214 ft^2 of conditioned space. Its HVAC system consists of three air handling units (AHUs) with each one connected to multiple VAV boxes (w. reheat coils). The building has been post retrofitted since the beginning of 2013 with a new building management system (BMS) from Automated Logic (ALC) and can be monitored remotely through its WebCTRL interface. Each AHU's cooling is provided by a direct expansion (DX) system with an outdoor condensing unit. This work focuses on the optimal control of AHU3 and its associated VAV boxes. AHU3 serves the north wing of the building which includes 10 zones (10 VAVs) spanning three floors.

Figure 1: WebCTRL view of Building 101 zones

To facilitate the control override implementation, we modified the WebCTRL interface to allow for real-time monitoring and contingency human intervention should zone comfort violations or out-of-range operating points occur. As shown in Figure 2, the MPC algorithm is implemented in AMPL with an interface to the optimization solver IPOPT. MATLAB is used as an interface tool connecting AMPL, IPOPT and WebCTRL. The algorithm is implemented and executed remotely. It acquires real-time sensor readings and historical data points and, after computing optimal control inputs, writes the control setpoints back to WebCTRL, which in turn drives the corresponding equipment towards the desired setpoints.

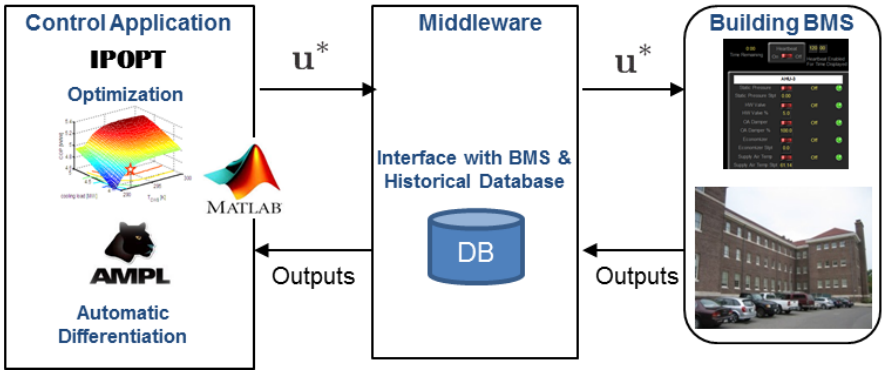

Figure 2: Framework of advanced building control architecture design and implementation

The energy-consuming components considered are the condensing unit (dual compressors with up to 6 stages total) in the DX system and the AHU supply fan. The implemented MPC algorithm uses weather forecast, predictions of zone temperature, and energy models to minimize energy consumption for AHU3 while maintaining occupants' comfort. There was no heating request during our demonstration period given the current building operating conditions and thus VAV reheat coils remained off.

3. MPC ALGORITHM DEVELOPMENT AND IMPLEMENTATION

In this section, we present details of the MPC algorithm development and implementation in Building 101. The details about model identification and calibration, algorithm architecture and implementation will be given as follows.

a. Building Thermal Zone and HVAC Models

To enable MPC design we first developed control-oriented mathematical models that could capture building zone temperature dynamics (comfort), heat transfer, and the power consumption of HVAC equipment (energy). For building supervisory control it is well established that a clear time-scale separation exists: while the time constants of the zone temperatures range from ~15 minutes to 1 hour (mainly depending on the size of the zone) due to the nature of underlying physical processes (convection, mixing), temperature changes are much faster inside DX coils, heating coils, and electric fans. Therefore, we can adopt quasi-steady-state modeling approach to describe most HVAC equipment like DX coils, heating coils, mixing boxes, and electric fans and use dynamic models to capture the dominating zone temperature transients. The following two subsections are devoted to describing dynamic zone and steady-state HVAC equipment models respectively.

i. System Identification of Models of Thermal Zones

In this section we present identification of linear parametric models for thermal zones of Building 101. System identification is a commonly used systematic procedure to build mathematical models of dynamic systems from experimental input-output data. A complete procedure involves identification experiments (functional tests), data pre-processing, selection of the model structure and estimation of model parameters, and validation of the model predictions on a different data set. The above three parts will be elaborated respectively.

- **Functional test**: The purpose of the functional test is to inject excitation signals into the system and collect the resulting output signals, which reveal the key dynamical properties of the system. In our test, for each VAV box, we applied Pseudo Random Binary Sequence (PRBS) signals for VAV flow setpoints to excite the zone thermal dynamics.
- **Data pre-processing**: Data is smoothed out using low-pass filter to eliminate high-frequency noise.
- **Model structure and parameter identification**:
  Among several candidates for the zone thermal dynamics such as ARX (Autoregressive model with eXogenous input), ARMAX (Autoregressive–moving-average model with eXogenous inputs), BJ (Box-Jenkins), OE (Output-Error), and state-space models (Ljung, 1999) we choose the following state-space model form (Li *et al.*, 2013):

$$x(k+1) = Ax(k) + Bu(k) + B_w w(k) \quad (1)$$

$$T_z(k) = Cx(k) + Du(k) \quad (2)$$

where k is the current time step, $\hat{x}$ is the state vector, $u(k) = \begin{pmatrix} T_{sa}(k) \\ \dot{m}_{sa}(k) \end{pmatrix}$ is the input vector; T_{sa} and $\dot{m}_{sa}$ represent VAV supply air temperature and supply air flow rate respectively; T_z is the zone temperature; *A, B, C, D* are system matrices. The convective coupling between zones was not considered in the current state-space models i.e. each zone is treated as an individual entity. We assume the disturbance term *w* is from the outdoor air temperature (T_{oa}) only for simplicity.

The chosen model and the collected data were then used by the subspace identification algorithm to obtain system matrices. MATLAB system identification toolbox (Juditsky, 2007) was chosen as the main computational platform. The models were validated against the operational data as shown in Figure 3. One can clearly observe that the model agrees with the data well in the context of predictive controller design for temperature control in office buildings.

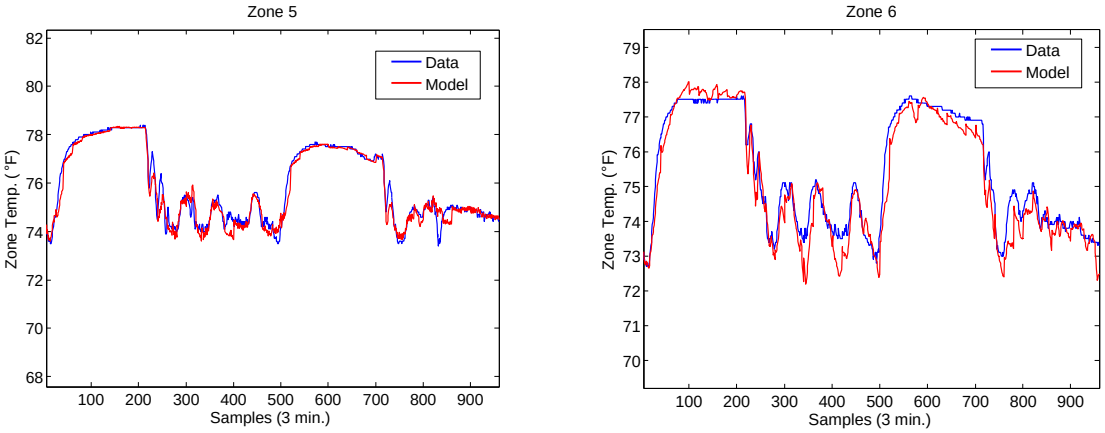

(a) Model validation results of zone 5 (b) Model validation results of zone 6

Figure 3: Selected zone model validation results

3.1.2 HVAC Equipment Models:

Table 1 summarizes the HVAC equipment models used in the MPC algorithm. For simplicity and computational efficiency, a polynomial model was developed to capture the compressors' power consumption of the direct expansion (DX) system. The limitation of our current DX energy prediction model lies in the fact that mixing humidity (inlet to AHU's evaporator coil) is not explicitly considered but is indirectly incorporated into the model coefficients. This modeling approach will not be valid if the AHU mixing humidity ratio changes significantly, which is not the case for the operation of this building. Future work is underway to address humidity (latent heat transfer) explicitly in our control-oriented model. Details about model calibration and validation for each component are omitted due to space limitations.

Table 1: HVAC Equipment Models

HVAC Subsystems	Assumptions & Notations	Equations
Outdoor air fraction and mixed-air temperature	Steady-state model as a function of outdoor air damper OAD: outdoor damper position T_{mix}: mixed air temperature T_{oa}: outdoor temperature T_{ra}: return air temperature $a_1, a_2 a_3$: model coefficients	$OAF = a_1 OAD^2 + a_2 OAD + a_3$ $T_{mix} = OAF T_{oa} + (1 - OAF) T_{ra}$
DX system model (compressor power)	Steady-state model as a function of air mass flow rate, mixed air and discharge air temperatures P_{DX}: power consumption T_{da}: discharge air temperature a, b, c, d, e, f: model coefficients	$P_{DX} = a + bL + cT_{da} + dLT_{da} + eL^2 T_{da} + fL^3, L = \Delta T \dot{m}_{da}$ $\Delta T = T_{mix} - T_{da}$
AHU supply air flow rate	Steady-state model of air flow leakage in the supply ducts to zone VAVs $\dot{m}^i_{vav}$: VAVi air mass flow	$\dot{m}_{da} = a \sum_{i=1}^{N_{vav}} \dot{m}^i_{vav} + b$

	N_{vav}: Number of VAV boxes a, b: model coefficients	
Electrical power of supply fan	Steady-state model as a function of supplied air flow P_{fan}: AHU fan power consumption a_1, a_2, a_3, a_4: model coefficients	$P_{fan} = a_1 \dot{m}_{da}{}^3 + a_2 \dot{m}_{da}{}^2 + a_3 \dot{m}_{da} + a_4$
Thermal power of VAV reheat coils	Steady-state model as a function of mass air flow rate, inlet and discharge air temperatures T_{da}^{AHU}: AHU discharge air temperature $T_{air,out}$: outlet air temperature c_{pa} : dry air specific heat c_{pw}: specific heat of water $\dot{m}_{sa}^{i}$: supply air mass flow of i[th] VAV box T_{wi}: VAV reheat coil inlet water temperature P_{reheat}^{i}: thermal power of i[th] VAV reheat coil a_1, a_2, a_3: model coefficients	$T_{air,out} = T_{da}^{AHU} + \frac{a_1 c_{pw} T_{wi}}{c_{pa} \dot{m}_{sa}^{a_2}} \alpha_{RHV}^{a_3}$ $P_{reheat}^{i} = \dot{m}_{sa}^{i} c_{pa} \left(T_{da}^{i} - T_{sa}^{AHU}\right)$

3.2 State Estimation: Kalman Filter

At each time step of the MPC algorithm, a state estimation algorithm is needed to obtain an initial estimation of zone temperature prior to predictions over a fixed time horizon. Following the simulation-based MPC study conducted previously in Li *et al.* (2013), a Luenberger observer was initially adopted for this purpose. However, it has been observed from operational data that the Luenberger observer tends to over-estimate, hence it often leads to false "comfort violation" prediction when the zone temperature is very close to the upper bound but still inside the comfort band. To account for this, a Kalman filter is adopted for more accurate state estimation.

The Kalman Filter is implemented following its standard form (Kailath, 2000):

1. *A-priori* state estimate : $\hat{x}_{k|k-1} = A\,\hat{x}_{k-1|k-1} + Bu_k$
2. *A-priori* error covariance : $P_{k|k-1} = AP(k-1)A^{\top}$+Q
3. A-priori output estimation error: $\tilde{T}_z(k) = T_z(k) - C\,\hat{x}_{k|k-1}$
4. Residual covariance: $S_k = CP_{k|k-1}C^{\top} + R$
5. Optimal Kalman gain: $K_k = P_{k|k-1}C^{\top}S_k^{-1}$
6. *A-posteriori* state estimation: $\hat{x}(k) = \hat{x}_{k|k-1} + K_k\,\tilde{T}_z(k)$
7. *A-posteriori* estimation error covariance : $P(k) = (I - K_k C)P_{k|k-1}$

The state estimation $\hat{x}(k)$ is used in MPC algorithm.

3.3 MPC Problem Formulation

Figure 4 shows the block diagram for the signal flows among major components of the BMS interface, Kalman Filter state estimator, and MPC controller. $T_z(k)$ and $\hat{T}_z(k)$ stand for the real-time and estimated temperature measurement for each zone, respectively. $\hat{x}(k)$ stands for the state-estimation obtained from Kalman Filter, which has been introduced above. The MPC algorithm calculates the optimal control input vector $u^*(k)$ as control setpoins. The control setpoints are updated every three minutes and the prediction horizon is set to two hours.

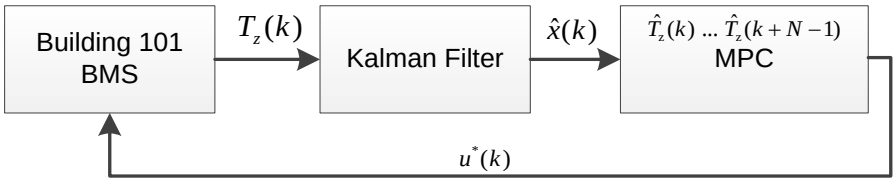

Figure 4: Schematic of MPC controller interacted with building BMS via state estimation

In this section we describe the MPC algorithm implemented as shown in Figure 5. In particular, we present the details of the constraints on decision variables and the optimality criterion (the cost).

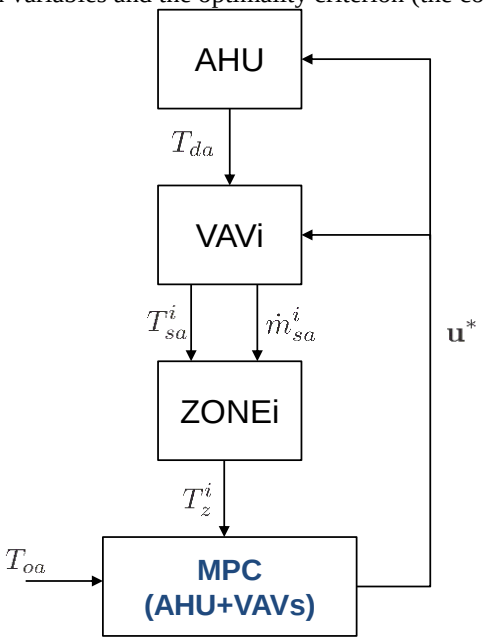

Figure 5: Schematic of interactions of AHU, VAVs, zones with the proposed MPC controller

The following presents the problem formulation of our proposed MPC algorithm. At each discrete time step k, the following constrained finite-time N-step optimal control problem is solved:

$$\boldsymbol{u}^{*} = \text{argmin}_{\mathbf{u}} \sum_{k=0}^{N-1} \ell_k \left(\hat{\boldsymbol{x}}_{t+k}, \boldsymbol{T}_{\boldsymbol{z}_{t+k}}, \boldsymbol{w}_{t+k}, \boldsymbol{u}_{t+k}\right) \tag{3}$$

$$\text{subj. to} \quad \hat{\boldsymbol{x}}(k+1) = \boldsymbol{A}\hat{\boldsymbol{x}}(k) + \boldsymbol{B}\boldsymbol{u}(k) + \boldsymbol{B}_{\boldsymbol{w}}\boldsymbol{w}(k) \tag{4}$$

$$\boldsymbol{T}_{\boldsymbol{z}}(k) = \boldsymbol{C}\hat{\boldsymbol{x}}(k) + \boldsymbol{D}\boldsymbol{u}(k) \tag{5}$$

$$\left(\boldsymbol{T}_{\boldsymbol{z}_{t+k}}, \boldsymbol{u}_{t+k}\right) \in \mathcal{C}_{t+k}, \quad k = 0, 1, 2, \dots, N \tag{6}$$

where Equation (4-6) represent the extended version of the system of equations for all zones and bold symbols represent the corresponding vector and system matrices. The stage cost $\ell_k(\cdot)$ in equation (3) consists of three components:

$$\ell_k(\hat{\boldsymbol{x}}_{\boldsymbol{t+k}}, \boldsymbol{T}_{\boldsymbol{z}_{t+k}}, \boldsymbol{w}_{t+k}, \boldsymbol{u}_{t+k}) = \ell_k^{pow}(\boldsymbol{u}_{t+k}, \boldsymbol{T}_{\boldsymbol{z}_{t+k}}, \boldsymbol{w}_{t+k}) + \ell_k^{constr}(\boldsymbol{T}_{\boldsymbol{z}_{t+k}}) + \ell_k^{\Delta}(\boldsymbol{u}_{t+k}, \boldsymbol{U}_{t+k}^{-}). \tag{7}$$

The first term $\ell_k^{pow}\left(\boldsymbol{u}_{t+k}, \boldsymbol{T}_{\boldsymbol{z}_{t+k}}\right)$ reflects the primary objective of the control algorithm to minimize the overall power consumption needed for cooling the air in the thermal zones, which contains the supply fan power, the compressor power from DX unit, and VAV reheat coil heat transfer rate. This cost function term is scaled to represent primary energy source consumption. The control input rate is penalized by:

$$\ell_k^{\Delta}(\boldsymbol{u}_{t+k}, \boldsymbol{U}_{t+k}^{-}) = \alpha \sum_{j=1}^{N} \left|\boldsymbol{u}_{t+k+j-1} - \boldsymbol{u}_{t+k+j}\right| \tag{8}$$

where $\boldsymbol{U}_{t+k}^{-} = (\boldsymbol{u}_{t+k-1}, \dots, \boldsymbol{u}_{t+k-N})$ and the weighting factor $\alpha > 0$ can be adjusted as needed.

The second term of the stage cost $\ell_k^{constr}(\cdot)$ is a penalty term for the violation of bounds on zone temperature (T_z). Instead of strictly enforcing a constraint such as $\boldsymbol{T}_{\boldsymbol{z}} \in [\boldsymbol{T}_{\boldsymbol{z}}^{\min}, \boldsymbol{T}_{\boldsymbol{z}}^{\max}]$, we introduce a "slack" variable $\boldsymbol{s}_k$ $\left(s_k^i \geq 0\right)$ and the following constraints were formulated:

$$\boldsymbol{T}_{\boldsymbol{z}} - \boldsymbol{T}_{\boldsymbol{z}}^{\max} \leq \boldsymbol{s}_k, \;\; \boldsymbol{T}_{\boldsymbol{z}}^{\min} - \boldsymbol{T}_{\boldsymbol{z}} \leq \boldsymbol{s}_k. \tag{10}$$

Violations of constraints on the T_z are penalized by augmenting the stage cost with a quadratic term:

$$\ell_k^{constr} = g_k \|\boldsymbol{s}_k\|^2 \quad (11)$$

where $g_k > 0$ is a tuning parameter. The convex set $\mathcal{C}_{t+k}$ is determined by the operating range of temperature and air flow rate. Note that the VAV reheat coils were not turned on during the demonstration period given the current building operation conditions which leads to $T_{da} = T_{sa}^i$.

4. EXPERIMENT RESULT AND PRELIMINARY PERFORMANCE ANALYSIS

The MPC testing period was conducted from September through November 2013. The algorithm was executed alternately with the baseline algorithm (currently implemented as part of the BMS) in order to generate sufficient data for performance comparison. This demonstration plan was chosen to mitigate the lack of sufficient baseline data caused by the AHU's DX coil operation with an inadequate refrigerant level until June 2013.

To evaluate the performance of the implemented MPC algorithm, preliminary analysis and comparison were conducted based on identifying similar outdoor air temperature (OAT) profile patterns between a selected MPC day and available baseline days. Ideally, more consideration such as outdoor air relative humidity (RH) and internal load should be given when selecting similar days to compare. However, due to limited number of available baselines due to the challenges mentioned above we decided to use outdoor temperature as the only selection criteria. Future work will be conducted to include other factors when more baseline data could be collected. Further work will also investigate the use of statistical comparisons with larger data-sets.

Figure 6 shows an example MPC day versus baseline day selected based on the similarity of OAT pattern (comparing computed correlation coefficient and mean temperature differences).

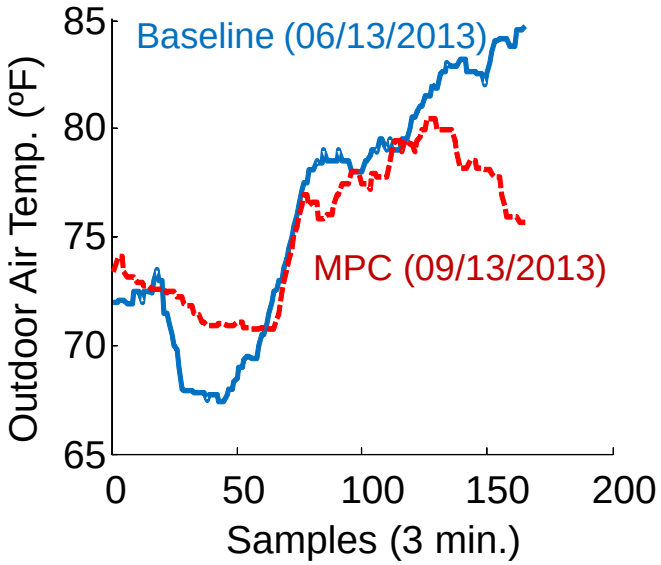

Figure 6: Comparison of outdoor air temperature pattern between baseline and MPC day

Figure 7 shows the comparisons of zone temperature between an example MPC day (09/13/2013) and the corresponding heuristic-based baseline day (06/13/2013). It can be observed that MPC controlled the temperature of all zones tightly around the upper comfort bound (75ºF) and thus yielded better thermal comfort relative to the post-BMS-retrofit heuristic-based control baseline.

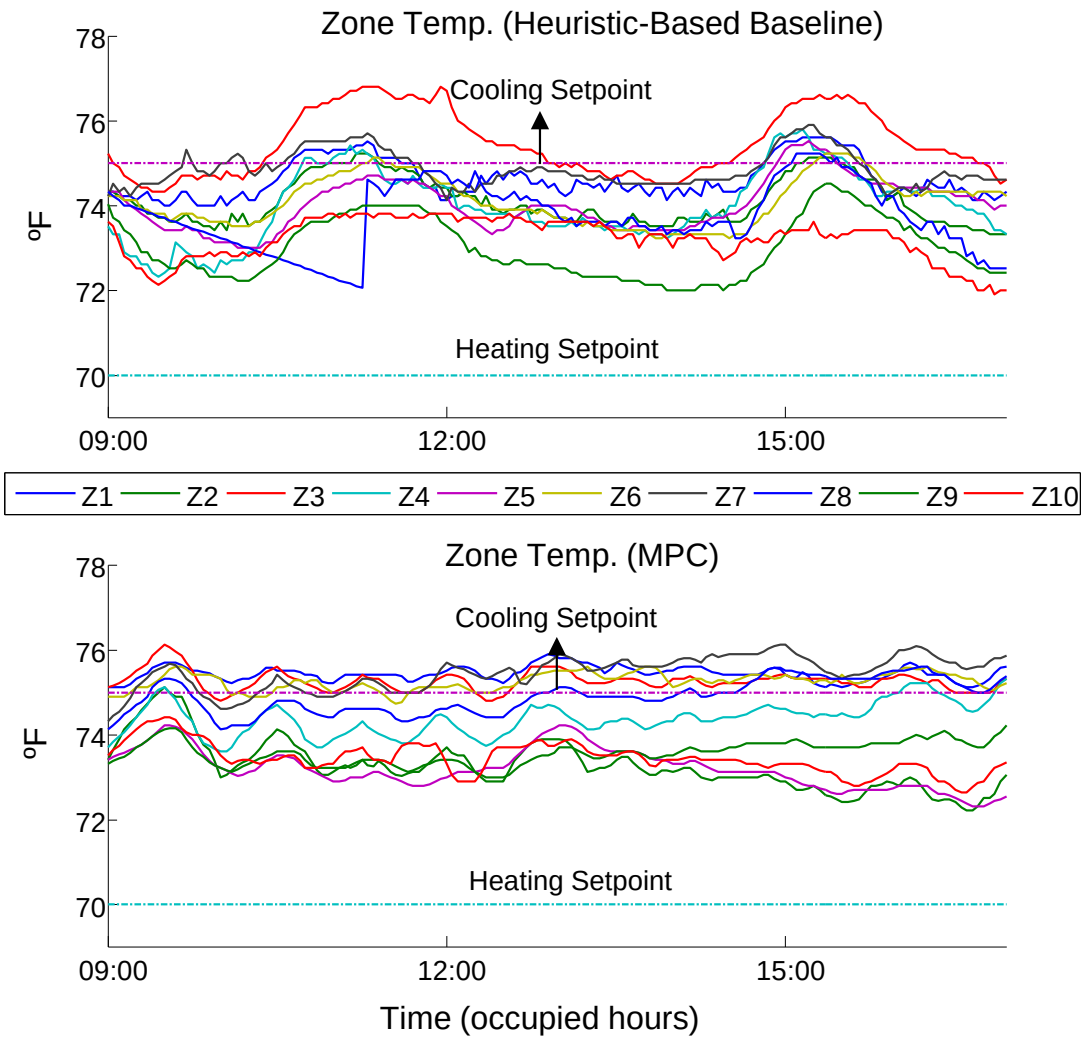

Figure 7: Comparisons of zone temperature between an example MPC day and heuristic-based baseline day.

As can be seen from Figure 8, MPC algorithm consumed less compressor power as a result of commanding a higher average supply air temperature setpoint. However, to maintain the zone temperature around the upper comfort bound, some zones require higher flow setpoints and thus resulted in overall higher average fan power.

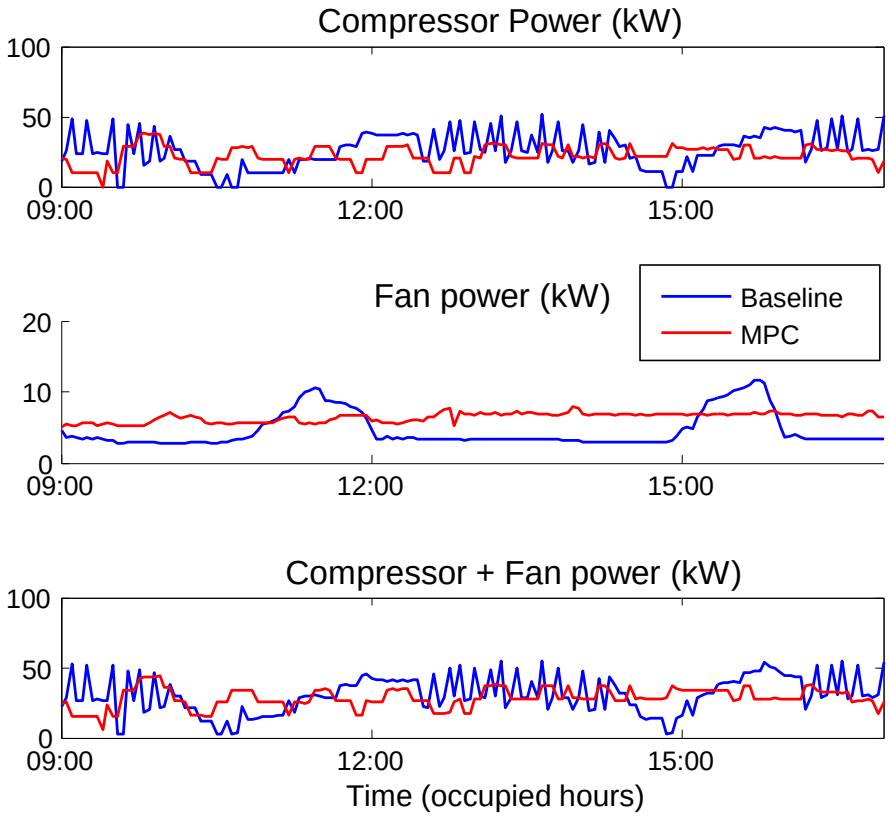

Figure 8: Comparisons of DX compressor power, fan power and total power between an example MPC day and heuristic-based baseline day.

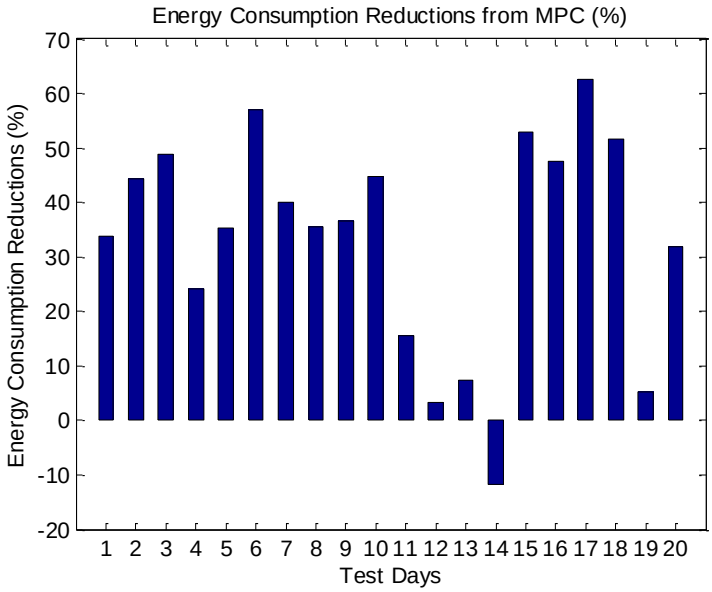

Figure 9: Energy savings obtained from 20 MPC test days (OAT-based comparison)

Figure 9 shows the MPC perfromance evaluation (energy consumption reductions) over 20 MPC test days by comparing each MPC test day with a correponsding baseline day selected based on similar OAT patterns. For the 20 MPC test days executed the average HVAC energy savings was 33% with 75% of test days exceeding energy savings of 20%.

5. CONCLUSIONS

In this study, functional tests were performed on AHU and VAV multi-zone system for system identification to extract control-oriented dynamic zone models and HVAC equipment models. In particular, low-order state-space models were identified from the designed input-output responses of thermal zones with disturbances from outdoor air conditions. The HVAC models were treated as quasi-steady-state with coefficients extracted from functional test data. A receding-horizon scheme was then designed and utilized the identified state-space models to predict the zone temperature responses and optimize a nonlinear energy and comfort based cost function to maintain the temperature of each zone within prescribed comfort bound and to simultaneously reduce the overall AHU's energy consumption based on HVAC models. The performance of the implemented MPC algorithm was estimated relative to baseline days (heuristic-based control) with similar outdoor air temperature patterns during the cooling and shoulder seasons and it was observed that MPC reduced the total electrical energy consumption by more than 20% on average while improving thermal comfort in terms of zone temperature and maintaining similar zone CO_2 levels. Future work is suggested for statistics-based performance evaluation.

ACKNOWLEDGEMENT

This work is funded by Consortium for Building Energy Innovation (formally known as Energy Efficient Buildings Hub), sponsored by the Department of Energy under Award Number DE-EE0004261. The authors are grateful to Hayden Reeve for managing the demonstration activities as well as his technical insights and valuable inputs to improve the paper and Timothy Wagner for his project management and supervision. We also thank Ken Kozma from Radius Systems for his technical support on WebCTRL during our advanced controls demonstration.

DISCLAIMER

REFERENCES

DOE, Building Energy Data Book, 2011, cited from http://buildingsdatabook.eren.doe.gov.

Brambley MR, P Haves, SC McDonald, P Torcellini, DG Hansen, D Holmberg, and K Roth, 2005, Advanced Sensors and Controls for Building Applications: Market Assessment and Potential R&D Pathways. *PNNL-15149*, Pacific Northwest National Laboratory, Richland, WA.

Katipamula S, RM Underhill, JK Goddard, DJ Taasevigen, MA Piette, J Granderson, RE Brown, SM Lanzisera, and T Kuruganti. 2012, Small- and Medium-Sized Commercial Building Monitoring and Controls Needs: A Scoping Study. *PNNL-22169*, Pacific Northwest National Laboratory, Richland, WA.

Qin, S. Joe, and Thomas A. Badgwell. "A survey of industrial model predictive control technology." *Control engineering practice* 11.7 (2003): 733-764.

Gayeski, N.T., 2010, Predictive Pre-Cooling Control for Low Lift Radiant Cooling using Building Thermal Mass, Ph.D. thesis, Massachusetts Institute of Technology.

Široký, J., Oldewurtel, F., Cigler, J., Prívara, S., Experimental analysis of model predictive control for an energy efficient building heating system, vol. 88, no. 9, p. 3079-3087

Narayanan, S., Wireless Platform for Energy-Efficient Building Control Retrofits, poster session presented at the *The Partners in Environmental Technology Technical Symposium & Workshop*, no. 64, p. F-84., Nov. 2011, Washington, D.C.

Bengea, S., Kelman, A., Borrelli, F., Taylor, R., and Narayanan, S., 2014, "Implementation of model predictive control for an HVAC system in mid-size commercial building", Journal of HVAC & R Research, Volume 20, Issue 1, pp. 121-135, 2014.

West, S. R., Ward, J. K., and Wall, J., 2014, Trial Results from a Model Predictive Control and Optimisation System for Commercial Building HVAC. Energy and Buildings.

May-Ostendorp, P. T., Henze, G. P., Rajagopalan, B., and Kalz, D., 2013, Experimental investigation of model predictive control-based rules for a radiantly cooled office. HVAC&R Research, 19(5), 602-615.

Li, P., Baric, M., Narayanan, S., and Yuan, S. 2012, A Simulation-Based Study of Model Predictive Control in a Medium-Sized Commercial Building, *2nd International High Performance Buildings Conference at Purdue*, July 16-19, 2012, West Lafayette, IN.

Ljung, L., 1999, *System Identification: Theory for the User*. Prentice Hall, 2nd edition.

Juditsky, A., Ljung, L., Zhang, Q., and Linskog, P., 2007, *System identification toolbox 7.0-Matlab*, Software MathWorks.

Li, P., O'Neill, Z.D., Braun, J.E., 2013, Development of Control-Oriented Models for Model Predictive Control in Buildings, *ASHRAE 2013 Annual Conference, June 22-26*, Denver, CO.

Kailath, T., Sayed, A. H., & Hassibi, B., 2000, *Linear Estimation*.